Bootstrapping Elliptic Feynman Integrals Using Schubert Analysis

Roger Morales[ORCID],[1] Anne Spiering[ORCID],[1] Matthias Wilhelm[ORCID],[1] Qinglin Yang (杨清霖)[ORCID],[2] and Chi Zhang (张驰)[ORCID][1]

[1]*Niels Bohr International Academy, Niels Bohr Institute, Copenhagen University, Blegdamsvej 17, 2100 Copenhagen Ø, Denmark*
[2]*CAS Key Laboratory of Theoretical Physics, Institute of Theoretical Physics, Chinese Academy of Sciences, Beijing 100190, China*

The symbol bootstrap has proven to be a powerful tool for calculating polylogarithmic Feynman integrals and scattering amplitudes. In this Letter, we initiate the symbol bootstrap for elliptic Feynman integrals. Concretely, we bootstrap the symbol of the twelve-point two-loop double-box integral in four dimensions, which depends on nine dual-conformal cross ratios. We obtain the symbol alphabet, which contains 100 logarithms as well as nine simple elliptic integrals, via a Schubert-type analysis, which we equally generalize to the elliptic case. In particular, we find a compact, one-line formula for the (2,2) coproduct of the result.

Introduction.—Within the framework of perturbative quantum field theory (QFT), precision predictions are expressed in terms of Feynman integrals, which evaluate to complicated transcendental numbers and functions.

In the last decade, much progress has been made for Feynman integrals, scattering amplitudes, as well as further quantities that belong to the simplest such class of functions, namely multiple polylogarithms (MPLs) [1–7]. This progress is to a large extent due to the excellent understanding we have of these functions, in particular through the so-called symbol [8–11]. The symbol allows one to decompose MPLs in terms of much simpler symbol letters $\log(\phi_i)$, where ϕ_i is a rational or algebraic function of the kinematics, and thus captures their singularity structure. Moreover, via the larger coproduct structure it is part of, the symbol can be used to reconstruct the function.

Among the most powerful techniques we have for MPLs is the so-called symbol bootstrap; see, e.g., Ref. [12] for a review. Since the symbol manifests the identities between MPLs via the known identities of the symbol letters $\log(\phi_i)$, it makes it possible to construct a basis for the space of functions in which a quantity must live. One can then make an ansatz and determine the corresponding coefficients via physical constraints. This idea has been successfully applied to scattering amplitudes [13–25], form factors [26–30], soft anomalous dimensions [31,32], and various individual Feynman integrals [33,34]. A crucial ingredient for the symbol bootstrap, though, is a good guess for the set of symbol letters, called the symbol alphabet. In a growing number of cases, it can be obtained via cluster algebras and tropical Graßmannians [23,35–58] as well as, more recently, a Schubert analysis [59–61], i.e., by analyzing the geometry of leading singularities in twistor space.

However, also more complicated classes of functions than MPLs occur in QFT in general and Feynman integrals in particular; see Ref. [62] for a review. The simplest of these are elliptic generalizations of multiple polylogarithms (eMPLs), for which there has been much recent progress [63–86]. Specifically, a symbol has been defined for eMPLs [78], the identities between elliptic symbol letters $\Omega^{(j)}(\tilde{\phi}_i)$ were understood [87], and the symbol of the first elliptic Feynman integrals was studied, revealing surprisingly simple structures [87,88].

In this Letter, we initiate the symbol bootstrap for elliptic Feynman integrals. Concretely, as a proof of principle, we calculate the twelve-point two-loop double-box integral with massless internal propagators in four spacetime dimensions; see Fig. 1. This diagram is an essential element in the basis for planar two-loop Feynman integrals [89]; in particular, it contributes to scattering amplitudes in the maximally supersymmetric Yang-Mills ($\mathcal{N} = 4$ sYM) theory [90] and, through its dual graph, to correlation functions in that theory as well as its conformal fishnet limit [91–93]. Our bootstrap is based on the structures that were observed in the ten-point elliptic double-box integral [88]—in particular the symbol prime [87]—as well as on generalizing the Schubert analysis to the elliptic case.

Setup.—We consider the twelve-point double-box integral

$$I_{\text{⧓}} = \int \frac{d^4x_0\, d^4x_{0'}}{x_{10}^2 x_{20}^2 x_{30}^2 x_{00'}^2 x_{40'}^2 x_{50'}^2 x_{60'}^2} \frac{x_{13}^2 x_{25}^2 x_{46}^2}{\,}, \qquad (1)$$
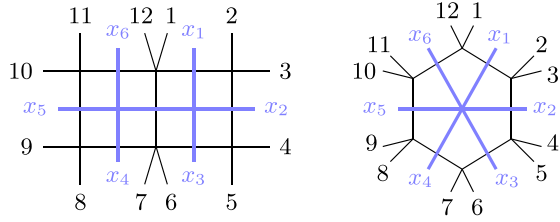
FIG. 1. The twelve-point elliptic double box and the related hexagon, as well as their dual graphs. The dual momenta are defined via $x_{i+1} - x_i = p_{2i} + p_{2i+1}$.

with the dual momentum x_i defined in Fig. 1 and $x_{ij}^2 \equiv (x_i - x_j)^2$ [94]. The double-box integral (1) depends on nine independent dual-conformal cross ratios,

$$\chi_{ab} = \chi_{ba} = x_{ba-1;ab-1} \quad \text{with} \quad x_{ij;kl} = \frac{x_{ij}^2 x_{kl}^2}{x_{ik}^2 x_{jl}^2}, \quad (2)$$

where a, b are nonadjacent in the cycle $\{1, \dots, 6\}$. Moreover, it satisfies a first-order differential equation relating it to the one-loop hexagon integral in six dimensions [95,96]:

$$\partial_{\chi_{14}} I_{\maltese} = \frac{1}{\sqrt{-\Delta_6}} I_{\maltese}, \quad (3)$$

where the normalized six-point Gram determinant $\Delta_6 = \det(x_{ij}^2)/(x_{14}^2 x_{25}^2 x_{36}^2)^2$ is a cubic polynomial in χ_{14}, showing that the symbol of the double-box integral is elliptic [97].

We are interested in the singularity structure of the integral in Eq. (1), i.e., its *symbol* [9,78,98], which can be obtained by taking the total differential recursively,

$$dI = \sum_i I_i dA_i \Rightarrow \mathcal{S}(I) = \sum_i \mathcal{S}(I_i) \otimes A_i, \quad (4)$$

where I, I_i, and the *symbol letters* A_i are n-, $(n-1)$-, and onefold integrals, respectively. We refer to the number of entries as length. It was computed in Ref. [88] and further indicated in Ref. [87] that the symbol of the ten-point double-box integral, given by the limit $x_{16}^2 \to 0$ and $x_{34}^2 \to 0$ of Eq. (1), respects the following simple structure:

$$\mathcal{S}\left(\frac{2\pi i}{\omega_1} I_{\maltese}\right) = \sum_{ikl} C^{ikl} \log(\phi_k) \otimes \log(\phi_l)$$

$$\otimes \left[\sum_j \log(\phi_{ij}) \otimes (2\pi i \, w_{c_j}) + \Omega_i \otimes (2\pi i \, \tau)\right], \quad (5)$$

where ω_1 and ω_2 are the periods of the elliptic curve, with modular parameter $\tau = \omega_2/\omega_1$, and $C^{ijk} \in \mathbb{Q}$. The symbol letters in the last entry are elliptic integrals $w_c = (1/\omega_1) \int_{-\infty}^{c} dx/y$, with $y^2 = -\Delta_6(x)$ defining the

elliptic curve [99]. Using the symbol prime [87], the remaining elliptic letters Ω_i can be obtained from the previous letters as

$$\Omega_i = \sum_j \partial_\tau \int_\gamma (2\pi i w_{c_j}) d\log(\phi_{ij}), \quad (6)$$

where the integration contour γ is independent of τ.

It is as yet unknown how to evaluate the twelve-point double-box integral in terms of eMPLs and then compute its symbol. The main obstacle in applying techniques such as differential equations or direct integration is the occurrence of excessive square roots. This can be anticipated from Eq. (3) as the symbol of the hexagon [100],

$$\mathcal{S}(I_{\maltese}) = \sum_{i<j} \mathrm{Box}_{ij} \otimes \log R_{ij}, \quad R_{ij} = \frac{\mathcal{G}_j^i - \sqrt{-\mathcal{G}_{ij}\mathcal{G}}}{\mathcal{G}_j^i + \sqrt{-\mathcal{G}_{ij}\mathcal{G}}}, \quad (7)$$

contains square roots of 16 different Gram determinants! Here Box_{ij} refers to the symbol of the four-mass box integral

$$\mathrm{Box}_{ij} = \log v_{ij} \otimes \log \frac{z_{ij}}{\bar{z}_{ij}} - \log u_{ij} \otimes \log \frac{1 - z_{ij}}{1 - \bar{z}_{ij}}, \quad (8)$$

with $u_{ij} = x_{kl;mn}$ and $v_{ij} = x_{lm;nk}$ for $\{k, l, m, n\} = \{1, \dots, 6\} \backslash \{i, j\}$, as well as z_{ij} and $\bar{z}_{ij}$ being defined by $u_{ij} = z_{ij} \bar{z}_{ij}$ and $v_{ij} = (1 - z_{ij})(1 - \bar{z}_{ij})$. Moreover, we introduced the following notation for Gram determinants:

$$\mathcal{G}_B^A := (-1)^{\sum_{c \in \{A,B\}} c} \det x_{ab}^2 \quad \text{and} \quad \mathcal{G}_A := \mathcal{G}_A^A, \quad (9)$$

with $a \in \{1, \dots, 6\} \backslash \{A\}$ and $b \in \{1, \dots, 6\} \backslash \{B\}$ where A, B are indices of dual points as in Eq. (7); in particular, $\mathcal{G}$ is the six-point Gram determinant.

Symbol letters via a Schubert problem.—We now predict the symbol letters required for the bootstrap of integral (1) by using Schubert analysis. These letters include the logarithmic letters—in particular those indicated by the symbol of the one-loop hexagon, Eq. (7) through Eq. (3)—and the elliptic last entries, while the complicated letters Ω_i can be constructed from these via Eq. (6).

Schubert analysis works in twistor space $\mathbb{P}^3$ [101,102], where to each dual point $x_i^{\alpha\dot{\alpha}} = x_i^\mu \sigma_\mu^{\alpha\dot{\alpha}}$ is associated a line $(i) = (1, t, x_i^{1\dot{1}} + x_i^{1\dot{2}}t, x_i^{2\dot{1}} + x_i^{2\dot{2}}t)$, where the points are parametrized by t.

MPL letters from boxes: Let us begin by discussing the one-loop four-mass box integral, whose symbol is given in Eq. (8). To solve for the one-loop leading singularity of this integral, we send its four propagators to zero, i.e., $x_{i0}^2 = 0$. In momentum twistor space, this is equivalent to looking for a line (L) intersecting all four kinematics lines (i)
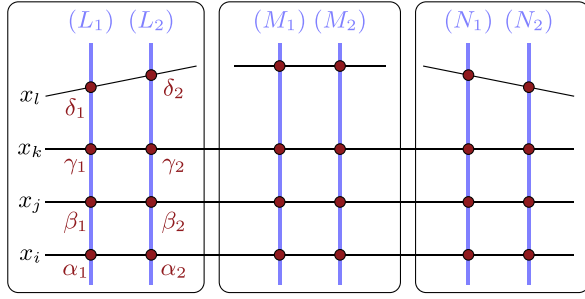
FIG. 2. Schubert problem providing the logarithmic letters in the symbol. The horizontal lines represent the external dual points x_i. The pair of vertical lines in each of the three boxes is uniquely determined by the intersection with the four corresponding external points. Logarithmic letters are obtained as cross ratios of the intersection points on a line.

simultaneously. There are exactly two solutions $(L_j)_{j=1,2}$ to this so-called Schubert problem. Each of these solutions has four distinct intersections with the four external lines [103,104], $\{\alpha_j, \beta_j, \gamma_j, \delta_j\}_{j=1,2}$; see Fig. 2. According to Ref. [60], one can form four multiplicatively independent cross ratios from these intersections,

$$z = \frac{(\alpha_1 - \beta_1)(\gamma_1 - \delta_1)}{(\alpha_1 - \gamma_1)(\beta_1 - \delta_1)}, \qquad \bar{z} = (1 \to 2), \quad (10)$$

as well as $(1 - z)$ and $(1 - \bar{z})$. Taking their products (quotients) we obtain the arguments of the letters for the first (second) entries of the four-mass box symbol (8). Since it contains only a single integration point corresponding to one loop momentum, we refer to this case as a "one-loop Schubert problem" in the following.

An interesting property of all known amplitudes and Feynman integrals in planar $\mathcal{N} = 4$ sYM theory [12,88,105–109], which arguably holds to all loop orders [110,111], is that their first two entries form the symbols of $\text{Li}_2(1 - x_{ab;cd})$, $\log(x_{ab;cd}) \log(x_{a'b';c'd'})$ or four-mass boxes whose symbol letters are $\{z, \bar{z}, 1 - z, 1 - \bar{z}\}$ or their degenerations for corresponding one-loop-box subdiagrams [112]. We assume that the twelve-point double-box integral (1) also *follows this pattern*. Since there are $\binom{6}{4} = 15$ four-mass box subtopologies, this gives us **9** candidates for the first entry and $30 + 9 = $ **39** candidates for the second entry.

Now we move to the third entries. In Ref. [60] it was realized that for certain two-loop planar Feynman integrals, the space of possible symbol letters in the third slot is generated by combining different one-loop Schubert problems and constructing cross ratios from the intersection points on the *external* lines. Here we refine this procedure as follows: in all known examples we observe that the required combined one-loop boxes share *three* external lines, and thus we assume this to also hold for the twelve-point double box; see Fig. 2. This requirement in particular

guarantees that the cross ratios formed on each line are the same. There are $\binom{6}{3} = 20$ such configurations in the double-box integral, each of them giving nine multiplicatively independent cross ratios. Taking the union of all cross ratios formed in this way, we find 104 multiplicatively independent letters: $9 \chi_{ab}$, $\mathcal{G}_{56}/(x_{13}^2 x_{24}^2)^2$ and its 14 images under the permutations S_6 of the external points x_i, the 15 last entries R_{ij} of the hexagon (7), five ratios of $\mathcal{G}_6/(x_{13}^2 x_{24}^2 x_{35}^2 x_{25}^2 x_{14}^2)$ to its five images under S_6, as well as 60 algebraic letters $(\mathcal{G}_{ij}^{ik} - \sqrt{\mathcal{G}_{ij}\mathcal{G}_{ik}})/(\mathcal{G}_{ij}^{ik} + \sqrt{\mathcal{G}_{ij}\mathcal{G}_{ik}})$. Combining them with the 30 ratios $\{z/\bar{z}, (1 - z)/(1 - \bar{z})\}$ from the second entries, we obtain **134** candidate third entries.

Elliptic Schubert analysis and last entries: So far, we have only constructed the arguments of the symbol letters $\log(\phi_i)$ through Schubert analysis, while, as indicated in Refs. [87,88], the counterparts of elliptic letters in MPL cases are logarithms rather than their arguments. However, one can also naturally construct logarithms in the above Schubert analysis; e.g., in the case in Eq. (10):

$$\log(z) = (\alpha_1 - \delta_1) \int_{\beta_1}^{\gamma_1} \frac{dx}{(x - \alpha_1)(x - \delta_1)}. \quad (11)$$

This is referred to as Aomoto polylogarithm [113–115]: two points on the line define the differential form (integrand), and the two other points define the integration range, while the normalization factor $\alpha_1 - \delta_1$ arises from the inverse of the contour integral

$$\frac{1}{\alpha_1 - \delta_1} = \frac{1}{2\pi i} \oint_{|x - \alpha_1| = \epsilon} \frac{dx}{(x - \alpha_1)(x - \delta_1)}, \quad (12)$$

which can also be understood as one period of the punctured sphere $\mathbb{C} \backslash \{\alpha_1, \delta_1\}$.

The above construction can be easily generalized to elliptic cases. Concretely, this amounts to considering the leading singularity of the two-loop double-box integral: the lines (0) and (0′) intersect each other as well as $\{(1),(2),(3)\}$ and $\{(4),(5),(6)\}$, respectively; see Fig. 3. Since this involves two integration points corresponding to two loop momenta at the same time, we refer to it as a "two-loop Schubert problem." It poses seven constraints on eight parameters and thus defines a curve, to which a one form is naturally associated. One can easily verify that this is an elliptic curve [116], and the elliptic generalization of Eq. (11) is

$$\frac{2\pi i}{\omega_1} \int_{\alpha}^{\beta} \frac{dx}{\sqrt{P(x)}}. \quad (13)$$

Here $dx/\sqrt{P(x)}$ is the differential form for the elliptic curve, with x parametrizing the points on any external line (i). Moreover, $2\pi i/\omega_1$ is the counterpart of Eq. (12) [117],
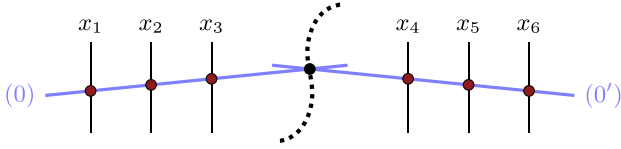
FIG. 3. Schubert problem providing the elliptic letters in the symbol. The horizontal lines, which intersect vertical lines corresponding to external points, intersect each other in an elliptic curve (the dotted curve; see also Ref. [116]). If the black point lies on an external line corresponding to the external point x_i, i.e., the elliptic curve intersects the external line in that black point, either (0) or (0′) satisfy the defining property of one of the vertical lines in Fig. 2 with external points x_i, x_1, x_2, x_3 or x_i, x_4, x_5, x_6, respectively. The corresponding intersection points yield the boundaries in the elliptic letters.

and $\{\alpha, \beta\}$ are intersections on (i) that stem from a one-loop Schubert problem including either $\{(1), (2), (3)\}$ or $\{(4), (5), (6)\}$. For instance, if we stick to the line (2) and choose the upper and lower bounds from $\{\alpha_1, \alpha_2\}$ in Fig. 2 with $\{i, j, k, l\} = \{1, 2, 3, 4\}$, the integral gives $w_{\chi_{14}}$, which will be one of our last entries. By going through all external lines and possible upper and lower bounds [118], we find **9** linear independent elliptic integrals which we assume to be the last entries of the twelve-point double-box integral.

Finally, let us remark that the eight letters besides $w_{\chi_{14}}$ can also be generated from the differential equation (3) as the values of χ_{14} for which the third letters R_{ij} in the hexagon become singular. In this way, we find an over-complete set of last entries, from which we construct a basis of nine last entries given by w_0, $w_{\chi_{14}}$, and τ and the six torus images w_{c_k}, where

$$c_k = \chi_{14} \frac{\mathcal{G}_i x_{ik}^4 + \mathcal{G}_j x_{jk}^4 + 2(\mathcal{G}_j^i + \mathcal{G}_{ij} x_{ij}^2) x_{ik}^2 x_{jk}^2}{2\mathcal{G}_{ij} x_{ij}^2 x_{jk}^2 x_{ik}^2}. \quad (14)$$

Here i and j are defined from the index k by identifying the set $\{i, j, k\}$ with (cyclic permutations of) $\{1, 2, 3\}$ or $\{4, 5, 6\}$. This basis spans the same space as the last entries obtained by the Schubert analysis. Note that there is an ambiguity in defining w_{c_k} due to the choice of $\pm y_{c_k}$. The choice used in this Letter is explicitly given in the Supplemental Material [118].

Bootstrap and results.—Let us now turn to the bootstrap of the twelve-point double-box symbol assuming the structure of Eq. (5); i.e., based on the alphabet generated in the previous section, we make an ansatz for the terms in the symbol whose last entry is not $2\pi i\tau$, while we assume that the terms with last entry $2\pi i\tau$ follow from those via Eq. (6).

A generic symbol $\sum_{i_1, \dots, i_n} C^{i_1, \dots, i_n} A_{i_1} \otimes \dots \otimes A_{i_n}$ does not correspond to the symbol of a function unless it satisfies the integrability condition [1]

TABLE I. Number of remaining free parameters after imposing each constraint.

Constraint	Free parameters
Alphabet	$\underbrace{9 \times 39 \times 134 \times 8}$
Integrability in slots 1 & 2	$\underbrace{60 \times 134 \times 8}$
Integrability in slots 3 & 4	$\underbrace{60 \times 19}$
Integrability in slots 2 & 3	1
Differential equation (3)	0

$$0 = \sum_{i_1, \dots, i_n} C^{i_1, \dots, i_n} A_{i_1} \otimes \dots \otimes A_{i_{p-1}} \otimes A_{i_{p+2}} \otimes \dots \otimes A_{i_n}$$
$$\times \left(\frac{\partial A_{i_p}}{\partial X_k} \frac{\partial A_{i_{p+1}}}{\partial X_m} - \frac{\partial A_{i_p}}{\partial X_m} \frac{\partial A_{i_{p+1}}}{\partial X_k} \right) \quad (15)$$

at all depths $1 \le p < n$, where $\{X_k\}$ are a set of independent kinematic parameters, e.g., $\{\chi_{ab}\}$ or $\{w_0, w_{\chi_{14}}, w_{c_k}, \tau\}$ for the double-box integral. In particular, in order to exploit the structure (5), we use the latter set of variables for integrability in entries three and four; see the Supplemental Material [118] for more details.

Amazingly, we find that imposing integrability uniquely fixes the symbol up to an overall constant, cf. Table I! We determine this constant via the differential equation (3), which moreover provides a consistency check. In addition, we checked that the symbol satisfies the conformal Ward identity [119] and the second-order differential equation of Refs. [120,121], and that it reduces to the known symbol of the ten-point double box [88] in the limit $x_{16}^2 \to 0$, $x_{34}^2 \to 0$. It also satisfies the (extended) Steinmann conditions [122–124] in all logarithmic symbol entries, i.e., discontinuities in overlapping channels vanish. Finally, the dual diagram of the double box is invariant under the $\mathbb{Z}_2$ reflection $x_i \to x_{7-i}$ and the permutations S_3 of $\{x_1, x_2, x_3\}$ (cf. Fig. 1), and this symmetry is manifest in our symbol result [125].

The full symbol of the twelve-point double-box integral can be written in terms of 100 logarithmic symbol letters and nine elliptic last letters, together with the structure shown in Eq. (6). We give its explicit form, as obtained from the bootstrap and organized by the last entries, in the Supplemental Material [118].

Reorganizing this symbol allows one to write the (2,2) coproduct of the double-box integral as a remarkably compact formula:

$$\Delta_{2,2} \left(\frac{2\pi i}{\omega_1} I_{\bowtie} \right)$$
$$= \sum_{i<j} \mathrm{Box}_{ij} \otimes \frac{2\pi i}{\omega_1} \int_{-\infty}^{\chi_{14}} \frac{d\chi'_{14} \log R_{ij}(\chi'_{14})}{\sqrt{-\Delta_6(\chi'_{14})}} - (\chi_{14} \to \infty), \quad (16)$$

where the limit in the second term is taken with all other eight χ_{ab}'s fixed. The first term in Eq. (16) manifests the differential equation (3) via Eq. (7), and the second (subtracted) term ensures integrability and that $I_{\text{⧓}}$ vanishes as $\chi_{14} \to \infty$. The explicit form of the subtracted terms as a tensor product of length-two functions can be understood as follows. Its first (length-two) entries can be easily obtained by taking the limit $\chi_{14} \to \infty$ in the four-mass box terms (8), e.g., $\text{Box}_{36} \to \mathcal{S}(\log x_{15;24} \log x_{14;25})$. In order to obtain the second (length-two) entries, we need to carefully define the integration contour connecting the two endpoints at infinity. This contour does not follow from the bootstrap, but is connected to the one in Eq. (6); we leave its investigation to future work.

The symbol of the second (length-two) entry in the (2,2) coproduct (16) can be written as

$$S_{ij} = \mathcal{S}\left(\frac{2\pi i}{\omega_1} \int \frac{d\chi'_{14} \log R_{ij}(\chi'_{14})}{\sqrt{-\Delta_6(\chi'_{14})}} \right) = \hat{S}_{ij} + \mathbf{\Omega}_{ij} \otimes 2\pi i\tau,$$

(17)

where $\mathbf{\Omega}_{ij}$ can be obtained by taking the τ derivative of the integral in Eq. (17), which is nothing but a realization of Eq. (6). The $\hat{S}_{ij}$ are given as follows: Taking i and j both from either $\{1, 2, 3\}$ or $\{4, 5, 6\}$, and k to be the respective third index from this set (with $\{i, j, k\}$ in cyclical ordering), then

$$\hat{S}_{ij} = \log R_{ij} \otimes 2\pi i w_{\chi_{14}} + \frac{1}{2} \log \frac{\mathcal{G}_j x_{jk}^4}{\mathcal{G}_i x_{ik}^4} \otimes 2\pi i w_{c_k}$$
$$- \frac{1}{2} \sum_{l \in \{i,j\}} \text{sgn}(k - l) \log \frac{\mathcal{G}_{ijk\backslash l}^{ij} - \sqrt{\mathcal{G}_{ij}\mathcal{G}_{ijk\backslash l}}}{\mathcal{G}_{ijk\backslash l}^{ij} + \sqrt{\mathcal{G}_{ij}\mathcal{G}_{ijk\backslash l}}} \otimes 2\pi i w_{c_l}.$$

(18)

Here, $\mathcal{G}_{ijk\backslash l} \equiv \mathcal{G}_{ik}$ if $l = j$ and $\mathcal{G}_{ijk\backslash l} \equiv \mathcal{G}_{jk}$ if $l = i$. If instead i and j take one value from each set, e.g., $i \in \{1, 2, 3\}$ and $j \in \{4, 5, 6\}$, then

$$\hat{S}_{ij} = \log R_{ij} \otimes 2\pi i w_{\chi_{14}}$$
$$+ \frac{(-1)^{i+j}}{2} \log \frac{z_{ij}^2 (1 - \bar{z}_{ij})}{\bar{z}_{ij}^2 (1 - z_{ij})} \otimes 2\pi i w_0$$
$$+ \sum_{l \notin \{i,j\}} \frac{(-1)^l}{2} \log \frac{\mathcal{G}_{mn}^{ij} - \sqrt{\mathcal{G}_{ij}\mathcal{G}_{mn}}}{\mathcal{G}_{mn}^{ij} + \sqrt{\mathcal{G}_{ij}\mathcal{G}_{mn}}} \otimes 2\pi i w_{c_l}, \quad (19)$$

where m and n are defined from l by identifying the set $\{l, m, n\}$ with (cyclic permutations) of $\{1, 2, 3\}$ or $\{4, 5, 6\}$. When taking the limit $\chi_{14} \to \infty$ to determine the subtracted term in Eq. (16), the six symbols (18) vanish while the nine symbols (19) yield four linearly independent combinations, resulting in the 19 integrable combinations found in Table I.

Conclusion and outlook.—In this Letter, we have initiated the symbol bootstrap for elliptic Feynman integrals. Concretely, we have determined the symbol of the two-loop twelve-point double-box integral. This calculation made use of two crucial ingredients: the simple structure (5) of the symbol in terms of the symbol prime and a Schubert analysis to predict the symbol letters. In particular, we show for the first time how a Schubert analysis can be used also to predict elliptic symbol letters. Amazingly, our assumptions on the symbol alphabet in the different entries combined with integrability were sufficient to uniquely determine the result up to an overall normalization, which we could fix via the differential equation (3)! Moreover, we found a very compact expression for the (2,2) coproduct, which in particular suggests that symbol-level integration [126] can be generalized to the elliptic case. For MPLs, it is well understood how to complete the symbol by boundary values at a base point to a form that allows for numerical evaluation, using the full coproduct [11]. In the present case, a similar form that yields numerics can be trivially obtained via the differential equation (3) from Refs. [95,96], whose right-hand side is known at full function level, and with boundary value $I_{\text{⧓}}|_{\chi_{14}=-\infty} = 0$.

We expect that the techniques developed in this work can be used to determine many further Feynman integrals and scattering amplitudes. A particular target would be all planar two-loop amplitudes in $\mathcal{N} = 4$ sYM theory, which can be expressed in terms of a finite basis of elliptic Feynman integrals using prescriptive unitarity [127]. Moreover, it would be interesting to make contact with the diagrammatic coaction [128,129] and spherical contours [115,130]. Many elliptic integrals that are relevant for LHC phenomenology contain massive internal propagators. It would be desirable to generalize the bootstrap approach and Schubert analysis also to this case. Finally, it would be very interesting to generalize the techniques developed here for elliptic integrals also to Feynman integrals containing higher-dimensional Calabi-Yau manifolds [62,116,131–137].

[1] K.-T. Chen, Iterated path integrals, Bull. Am. Math. Soc. **83**, 831 (1977).

[2] A. B. Goncharov, Geometry of configurations, polylogarithms, and motivic cohomology, Adv. Math. **114**, 197 (1995).

[3] A. B. Goncharov, Multiple polylogarithms, cyclotomy and modular complexes, Math. Res. Lett. **5**, 497 (1998).

[4] E. Remiddi and J. A. M. Vermaseren, Harmonic polylogarithms, Int. J. Mod. Phys. A **15**, 725 (2000).

[5] J. M. Borwein, D. M. Bradley, D. J. Broadhurst, and P. Lisonek, Special values of multiple polylogarithms, Trans. Am. Math. Soc. **353**, 907 (2001).

[6] S. Moch, P. Uwer, and S. Weinzierl, Nested sums, expansion of transcendental functions and multiscale multiloop integrals, J. Math. Phys. (N.Y.) **43**, 3363 (2002).

[7] J. Ablinger, J. Blümlein, and C. Schneider, Analytic and algorithmic aspects of generalized harmonic sums and polylogarithms, J. Math. Phys. (N.Y.) **54**, 082301 (2013).

[8] A. B. Goncharov, Galois symmetries of fundamental groupoids and noncommutative geometry, Duke Math. J. **128**, 209 (2005).

[9] A. B. Goncharov, M. Spradlin, C. Vergu, and A. Volovich, Classical Polylogarithms for Amplitudes and Wilson Loops, Phys. Rev. Lett. **105**, 151605 (2010).

[10] C. Duhr, H. Gangl, and J. R. Rhodes, From polygons and symbols to polylogarithmic functions, J. High Energy Phys. 10 (2012) 075.

[11] C. Duhr, Hopf algebras, coproducts and symbols: An application to Higgs boson amplitudes, J. High Energy Phys. 08 (2012) 043.

[12] S. Caron-Huot, L. J. Dixon, J. M. Drummond, F. Dulat, J. Foster, O. Gürdoğan, M. von Hippel, A. J. McLeod, and G. Papathanasiou, The Steinmann cluster bootstrap for $\mathcal{N} = 4$ super Yang-Mills amplitudes, Proc. Sci. CORFU2019 (**2020**) 003 [arXiv:2005.06735].

[13] L. J. Dixon, J. M. Drummond, and J. M. Henn, Bootstrapping the three-loop hexagon, J. High Energy Phys. 11 (2011) 023.

[14] L. J. Dixon, J. M. Drummond, and J. M. Henn, Analytic result for the two-loop six-point NMHV amplitude in $\mathcal{N} = 4$ super Yang-Mills theory, J. High Energy Phys. 01 (2012) 024.

[15] L. J. Dixon, J. M. Drummond, M. von Hippel, and J. Pennington, Hexagon functions and the three-loop remainder function, J. High Energy Phys. 12 (2013) 049.

[16] L. J. Dixon, J. M. Drummond, C. Duhr, and J. Pennington, The four-loop remainder function and multi-Regge behavior at NNLLA in planar $\mathcal{N} = 4$ super-Yang-Mills theory, J. High Energy Phys. 06 (2014) 116.

[17] L. J. Dixon and M. von Hippel, Bootstrapping an NMHV amplitude through three loops, J. High Energy Phys. 10 (2014) 065.

[18] J. M. Drummond, G. Papathanasiou, and M. Spradlin, A symbol of uniqueness: The cluster bootstrap for the 3-Loop MHV heptagon, J. High Energy Phys. 03 (2015) 072.

[19] L. J. Dixon, M. von Hippel, and A. J. McLeod, The four-loop six-gluon NMHV ratio function, J. High Energy Phys. 01 (2016) 053.

[20] S. Caron-Huot, L. J. Dixon, A. McLeod, and M. von Hippel, Bootstrapping a Five-Loop Amplitude Using Steinmann Relations, Phys. Rev. Lett. **117**, 241601 (2016).

[21] L. J. Dixon, M. von Hippel, A. J. McLeod, and J. Trnka, Multi-loop positivity of the planar $\mathcal{N} = 4$ SYM six-point amplitude, J. High Energy Phys. 02 (2017) 112.

[22] L. J. Dixon, J. Drummond, T. Harrington, A. J. McLeod, G. Papathanasiou, and M. Spradlin, Heptagons from the Steinmann cluster bootstrap, J. High Energy Phys. 02 (2017) 137.

[23] J. Drummond, J. Foster, Ö. Gürdoğan, and G. Papathanasiou, Cluster adjacency and the four-loop NMHV heptagon, J. High Energy Phys. 03 (2019) 087.

[24] S. Caron-Huot, L. J. Dixon, F. Dulat, M. von Hippel, A. J. McLeod, and G. Papathanasiou, Six-Gluon amplitudes in planar $\mathcal{N} = 4$ super-Yang-Mills theory at six and seven loops, J. High Energy Phys. 08 (2019) 016.

[25] L. J. Dixon and Y.-T. Liu, Lifting heptagon symbols to functions, J. High Energy Phys. 10 (2020) 031.

[26] A. Brandhuber, G. Travaglini, and G. Yang, Analytic two-loop form factors in $\mathcal{N} = 4$ SYM, J. High Energy Phys. 05 (2012) 082.

[27] L. J. Dixon, A. J. McLeod, and M. Wilhelm, A three-point form factor through five loops, J. High Energy Phys. 04 (2021) 147.

[28] Y. Guo, L. Wang, and G. Yang, Bootstrapping a Two-Loop Four-Point Form Factor, Phys. Rev. Lett. **127**, 151602 (2021).

[29] L. J. Dixon, O. Gürdoğan, A. J. McLeod, and M. Wilhelm, Bootstrapping a stress-tensor form factor through eight loops, J. High Energy Phys. 07 (2022) 153.

[30] L. J. Dixon, O. Gürdoğan, Y.-T. Liu, A. J. McLeod, and M. Wilhelm, Antipodal Self-Duality for a Four-Particle Form Factor, Phys. Rev. Lett. **130**, 111601 (2023).

[31] Y. Li and H. X. Zhu, Bootstrapping Rapidity Anomalous Dimensions for Transverse-Momentum Resummation, Phys. Rev. Lett. **118**, 022004 (2017).

[32] O. Almelid, C. Duhr, E. Gardi, A. McLeod, and C. D. White, Bootstrapping the QCD soft anomalous dimension, J. High Energy Phys. 09 (2017) 073.

[33] J. Henn, E. Herrmann, and J. Parra-Martinez, Bootstrapping two-loop Feynman integrals for planar $\mathcal{N} = 4$ sYM, J. High Energy Phys. 10 (2018) 059.

[34] S. He, Z. Li, and Q. Yang, Kinematics, cluster algebras and Feynman integrals, arXiv:2112.11842.

[35] J. Golden, A. B. Goncharov, M. Spradlin, C. Vergu, and A. Volovich, Motivic amplitudes and cluster coordinates, J. High Energy Phys. 01 (2014) 091.

[36] J. Golden and M. Spradlin, A cluster bootstrap for two-loop MHV amplitudes, J. High Energy Phys. 02 (2015) 002.

[37] J. Golden, M. F. Paulos, M. Spradlin, and A. Volovich, Cluster polylogarithms for scattering amplitudes, J. Phys. A **47**, 474005 (2014).

[38] J. Golden and M. Spradlin, An analytic result for the two-loop seven-point MHV amplitude in $\mathcal{N} = 4$ SYM, J. High Energy Phys. 08 (2014) 154.

[39] J. Drummond, J. Foster, and Ö. Gürdoğan, Cluster Adjacency Properties of Scattering Amplitudes in $\mathcal{N} = 4$ Supersymmetric Yang-Mills Theory, Phys. Rev. Lett. **120**, 161601 (2018).

[40] J. L. Bourjaily, A. J. McLeod, M. von Hippel, and M. Wilhelm, Rationalizing loop integration, J. High Energy Phys. 08 (2018) 184.

[41] J. Drummond, J. Foster, and Ö. Gürdoğan, Cluster adjacency beyond MHV, J. High Energy Phys. 03 (2019) 086.

[42] J. Golden and A. J. McLeod, Cluster algebras and the subalgebra constructibility of the seven-particle remainder function, J. High Energy Phys. 01 (2019) 017.

[43] J. Golden, A. J. McLeod, M. Spradlin, and A. Volovich, The Sklyanin bracket and cluster adjacency at all multiplicity, J. High Energy Phys. 03 (2019) 195.

[44] J. Golden and A. J. McLeod, The two-loop remainder function for eight and nine particles, J. High Energy Phys. 06 (2021) 142.

[45] J. Drummond, J. Foster, Ö. Gürdoğan, and C. Kalousios, Tropical Grassmannians, cluster algebras and scattering amplitudes, J. High Energy Phys. 04 (2020) 146.

[46] J. Drummond, J. Foster, O. Gürdogan, and C. Kalousios, Algebraic singularities of scattering amplitudes from tropical geometry, J. High Energy Phys. 04 (2021) 002.

[47] N. Arkani-Hamed, T. Lam, and M. Spradlin, Nonperturbative geometries for planar $\mathcal{N} = 4$ SYM amplitudes, J. High Energy Phys. 03 (2021) 065.

[48] N. Henke and G. Papathanasiou, How tropical are seven- and eight-particle amplitudes?, J. High Energy Phys. 08 (2020) 005.

[49] J. Drummond, J. Foster, O. Gürdogan, and C. Kalousios, Tropical fans, scattering equations and amplitudes, J. High Energy Phys. 11 (2021) 071.

[50] J. Mago, A. Schreiber, M. Spradlin, and A. Volovich, Symbol alphabets from plabic graphs, J. High Energy Phys. 10 (2020) 128.

[51] D. Chicherin, J. M. Henn, and G. Papathanasiou, Cluster Algebras for Feynman Integrals, Phys. Rev. Lett. **126**, 091603 (2021).

[52] J. Mago, A. Schreiber, M. Spradlin, A. Y. Srikant, and A. Volovich, Symbol alphabets from plabic graphs II: Rational letters, J. High Energy Phys. 04 (2021) 056.

[53] A. Herderschee, Algebraic branch points at all loop orders from positive kinematics and wall crossing, J. High Energy Phys. 07 (2021) 049.

[54] S. He, Z. Li, and Q. Yang, Notes on cluster algebras and some all-loop Feynman integrals, J. High Energy Phys. 06 (2021) 119.

[55] J. Mago, A. Schreiber, M. Spradlin, A. Yelleshpur Srikant, and A. Volovich, Symbol alphabets from plabic graphs III: $n = 9$, J. High Energy Phys. 09 (2021) 002.

[56] N. Henke and G. Papathanasiou, Singularities of eight- and nine-particle amplitudes from cluster algebras and tropical geometry, J. High Energy Phys. 10 (2021) 007.

[57] L. Ren, M. Spradlin, and A. Volovich, Symbol alphabets from tensor diagrams, J. High Energy Phys. 12 (2021) 079.

[58] G. Papathanasiou, Chapter 5: Analytic bootstraps for scattering amplitudes and beyond, J. Phys. A **55**, 443006 (2022).

[59] N. Arkani-Hamed, *Talk in The Conference Positive Geometries in Scattering Amplitudes and Beyond, Mainz Institute for Theoretical Physics* (2021), https://indico.mitp.uni-mainz.de/event/236/.

[60] Q. Yang, Schubert problems, positivity and symbol letters, J. High Energy Phys. 08 (2022) 168.

[61] S. He, J. Liu, Y. Tang, and Q. Yang, The symbology of Feynman integrals from twistor geometries, arXiv:2207.13482.

[62] J. L. Bourjaily *et al.*, Functions beyond multiple polylogarithms for precision collider physics, in *2022 Snowmass Summer Study* (2022), arXiv:2203.07088.

[63] S. Laporta and E. Remiddi, Analytic treatment of the two loop equal mass sunrise graph, Nucl. Phys. **B704**, 349 (2005).

[64] S. Muller-Stach, S. Weinzierl, and R. Zayadeh, From motives to differential equations for loop integrals, Proc. Sci. LL2012 (**2012**) 005 [arXiv:1209.3714].

[65] F. Brown and A. Levin, Multiple elliptic polylogarithms, arXiv:1110.6917.

[66] S. Bloch and P. Vanhove, The elliptic dilogarithm for the sunset graph, J. Number Theory **148**, 328 (2015).

[67] L. Adams, C. Bogner, and S. Weinzierl, The two-loop sunrise graph with arbitrary masses, J. Math. Phys. (N.Y.) **54**, 052303 (2013).

[68] L. Adams, C. Bogner, and S. Weinzierl, The two-loop sunrise graph in two space-time dimensions with arbitrary masses in terms of elliptic dilogarithms, J. Math. Phys. (N.Y.) **55**, 102301 (2014).

[69] L. Adams, C. Bogner, and S. Weinzierl, The two-loop sunrise integral around four space-time dimensions and generalisations of the Clausen and Glaisher functions towards the elliptic case, J. Math. Phys. (N.Y.) **56**, 072303 (2015).

[70] L. Adams, C. Bogner, and S. Weinzierl, The iterated structure of the all-order result for the two-loop sunrise integral, J. Math. Phys. (N.Y.) **57**, 032304 (2016).

[71] L. Adams, C. Bogner, A. Schweitzer, and S. Weinzierl, The kite integral to all orders in terms of elliptic polylogarithms, J. Math. Phys. (N.Y.) **57**, 122302 (2016).

[72] L. Adams and S. Weinzierl, Feynman integrals and iterated integrals of modular forms, Commun. Num. Theor. Phys. **12**, 193 (2018).

[73] L. Adams, E. Chaubey, and S. Weinzierl, Simplifying Differential Equations for Multiscale Feynman Integrals beyond Multiple Polylogarithms, Phys. Rev. Lett. **118**, 141602 (2017).

[74] C. Bogner, A. Schweitzer, and S. Weinzierl, Analytic continuation and numerical evaluation of the kite integral and the equal mass sunrise integral, Nucl. Phys. **B922**, 528 (2017).

[75] J. Broedel, C. Duhr, F. Dulat, and L. Tancredi, Elliptic polylogarithms and iterated integrals on elliptic curves. Part I: General formalism, J. High Energy Phys. 05 (2018) 093.

[76] J. Broedel, C. Duhr, F. Dulat, and L. Tancredi, Elliptic polylogarithms and iterated integrals on elliptic curves II: An application to the sunrise integral, Phys. Rev. D **97**, 116009 (2018).

[77] L. Adams and S. Weinzierl, The ε-form of the differential equations for Feynman integrals in the elliptic case, Phys. Lett. B **781**, 270 (2018).

[78] J. Broedel, C. Duhr, F. Dulat, B. Penante, and L. Tancredi, Elliptic symbol calculus: From elliptic polylogarithms to iterated integrals of Eisenstein series, J. High Energy Phys. 08 (2018) 014.

[79] J. Broedel, C. Duhr, F. Dulat, B. Penante, and L. Tancredi, Elliptic Feynman integrals and pure functions, J. High Energy Phys. 01 (2019) 023.

[80] I. Hönemann, K. Tempest, and S. Weinzierl, Electron self-energy in QED at two loops revisited, Phys. Rev. D **98**, 113008 (2018).

[81] C. Bogner, S. Müller-Stach, and S. Weinzierl, The unequal mass sunrise integral expressed through iterated integrals on $\bar{\mathcal{M}}_{1,3}$, Nucl. Phys. **B954**, 114991 (2020).

[82] J. Broedel, C. Duhr, F. Dulat, B. Penante, and L. Tancredi, Elliptic polylogarithms and Feynman parameter integrals, J. High Energy Phys. 05 (2019) 120.

[83] C. Duhr and L. Tancredi, Algorithms and tools for iterated Eisenstein integrals, J. High Energy Phys. 02 (2020) 105.

[84] M. Walden and S. Weinzierl, Numerical evaluation of iterated integrals related to elliptic Feynman integrals, Comput. Phys. Commun. **265**, 108020 (2021).

[85] S. Weinzierl, Modular transformations of elliptic Feynman integrals, Nucl. Phys. **B964**, 115309 (2021).

[86] M. Giroux and A. Pokraka, Loop-by-loop differential equations for dual (Elliptic) Feynman integrals, J. High Energy Phys. 03 (2023) 155.

[87] M. Wilhelm and C. Zhang, Symbology for elliptic multiple polylogarithms and the symbol prime, J. High Energy Phys. 01 (2023) 089.

[88] A. Kristensson, M. Wilhelm, and C. Zhang, Elliptic Double Box and Symbology beyond Polylogarithms, Phys. Rev. Lett. **127**, 251603 (2021).

[89] J. L. Bourjaily, E. Herrmann, and J. Trnka, Prescriptive unitarity, J. High Energy Phys. 06 (2017) 059.

[90] J. L. Bourjaily and J. Trnka, Local integrand representations of all two-loop amplitudes in planar SYM, J. High Energy Phys. 08 (2015) 119.

[91] O. Gürdoğan and V. Kazakov, New Integrable 4D Quantum Field Theories from Strongly Deformed Planar $\mathcal{N} = 4$ Supersymmetric Yang-Mills Theory, Phys. Rev. Lett. **117**, 201602 (2016).

[92] C. Sieg and M. Wilhelm, On a CFT limit of planar γ_i-deformed $\mathcal{N} = 4$ SYM theory, Phys. Lett. B **756**, 118 (2016).

[93] D. Grabner, N. Gromov, V. Kazakov, and G. Korchemsky, Strongly γ-Deformed $\mathcal{N} = 4$ Supersymmetric Yang-Mills Theory as an Integrable Conformal Field Theory, Phys. Rev. Lett. **120**, 111601 (2018).

[94] The numerator is chosen to render the diagram dual conformal invariant.

[95] M. F. Paulos, M. Spradlin, and A. Volovich, Mellin amplitudes for dual conformal integrals, J. High Energy Phys. 08 (2012) 072.

[96] D. Nandan, M. F. Paulos, M. Spradlin, and A. Volovich, Star integrals, convolutions and simplices, J. High Energy Phys. 05 (2013) 105.

[97] It can be seen from Eq. (3) that at least one last entry of the symbol is not a logarithm but an elliptic integral, cf. also Eq. (5).

[98] F. Brown, Notes on motivic periods, Commun. Num. Theory Phys. **11**, 557 (2017).

[99] Note that we are defining the elliptic curve via a cubic polynomial here, while it was defined via a quartic polynomial in Ref. [88]. The two curves are birational, though.

[100] M. Spradlin and A. Volovich, Symbols of one-loop integrals from mixed state motives, J. High Energy Phys. 11 (2011) 084.

[101] A. Hodges, Eliminating spurious poles from gauge-theoretic amplitudes, J. High Energy Phys. 05 (2013) 135.

[102] L. J. Mason and D. Skinner, Dual superconformal invariance, momentum twistors and Grassmannians, J. High Energy Phys. 11 (2009) 045.

[103] N. Arkani-Hamed, J. L. Bourjaily, F. Cachazo, and J. Trnka, Local integrals for planar scattering amplitudes, J. High Energy Phys. 06 (2012) 125.

[104] J. L. Bourjaily, S. Caron-Huot, and J. Trnka, Dual-conformal regularization of infrared loop divergences and the chiral box expansion, J. High Energy Phys. 01 (2015) 001.

[105] S. Caron-Huot, Superconformal symmetry and two-loop amplitudes in planar $\mathcal{N} = 4$ super Yang-Mills, J. High Energy Phys. 12 (2011) 066.

[106] S. He, Z. Li, and C. Zhang, The symbol and alphabet of two-loop NMHV amplitudes from $\bar{Q}$ equations, J. High Energy Phys. 03 (2021) 278.

[107] S. He, Z. Li, Q. Yang, and C. Zhang, Feynman Integrals and Scattering Amplitudes from Wilson Loops, Phys. Rev. Lett. **126**, 231601 (2021).

[108] Z. Li and C. Zhang, The three-loop MHV octagon from $\bar{Q}$ equations, J. High Energy Phys. 12 (2021) 113.

[109] S. He, Z. Li, and C. Zhang, A nice two-loop next-to-next-to-MHV amplitude in $\mathcal{N} = 4$ super-Yang-Mills, J. High Energy Phys. 12 (2022) 158.

[110] D. Gaiotto, J. Maldacena, A. Sever, and P. Vieira, Pulling the straps of polygons, J. High Energy Phys. 12 (2011) 011.

[111] S. He, Z. Li, and Q. Yang, Comments on all-loop constraints for scattering amplitudes and Feynman integrals, J. High Energy Phys. 01 (2022) 073; 05 (2022) 76.

[112] Conjecturally, this is true for finite planar Feynman integrals with massless propagators.

[113] K. Aomoto, Addition theorem of Abel type for hyperlogarithms, Nagoya Math. J. **88**, 55 (1982).

[114] A. B. Goncharov, A simple construction of Grassmannian polylogarithms, arXiv:0908.2238.

[115] N. Arkani-Hamed and E. Y. Yuan, One-loop integrals from spherical projections of planes and quadrics, arXiv:1712.09991.

[116] C. Vergu and M. Volk, Traintrack Calabi-Yaus from twistor geometry, J. High Energy Phys. 07 (2020) 160.

[117] Alternatively, one can choose $-(2\pi i)/\omega_2$ as the normalization factor, amounting to the corresponding alternative normalization of the elliptic Feynman integrals. Including such factors also ensures that the elliptic letters degenerate to logarithms in the kinematic limit where the elliptic curve degenerates. See Ref. [87] for further details.

[118] See Supplemental Material at http://link.aps.org/supplemental/10.1103/PhysRevLett.131.041601 dbSymbol.txt for a Mathematica-readable expression for the symbol result of the 12-point double box integral, and supp.pdf for the details of the Schubert analysis for the last entries, comments on integrability, and a compact expression for the symbol.

[119] D. Chicherin and E. Sokatchev, Conformal anomaly of generalized form factors and finite loop integrals, J. High Energy Phys. 04 (2018) 082.

[120] J. M. Drummond, J. Henn, V. A. Smirnov, and E. Sokatchev, Magic identities for conformal four-point integrals, J. High Energy Phys. 01 (2007) 064.

[121] J. M. Drummond, J. M. Henn, and J. Trnka, New differential equations for on-shell loop integrals, J. High Energy Phys. 04 (2011) 083.

[122] O. Steinmann, Über den Zusammenhang zwischen den Wightmanfunktionen und der retardierten Kommutatoren, Helv. Phys. Acta **33,** 257 (1960).

[123] O. Steinmann, Wightman-Funktionen und retardierten Kommutatoren. II, Helv. Phys. Acta **33,** 347 (1960).

[124] S. Caron-Huot, L. J. Dixon, F. Dulat, M. von Hippel, A. J. McLeod, and G. Papathanasiou, The cosmic Galois group and extended Steinmann relations for planar $\mathcal{N} = 4$ SYM amplitudes, J. High Energy Phys. 09 (2019) 061.

[125] This symmetry is lost in Eq. (1) due to the normalization factor in the numerator, but recovered in $I_{\text{⧲}}/\omega_1$ and hence in Eq. (16). We discuss the manifestation of these symmetries at the level of the symbol in more detail in Ref. [118].

[126] S. Caron-Huot and S. He, Jumpstarting the all-loop S-matrix of planar $\mathcal{N} = 4$ super Yang-Mills, J. High Energy Phys. 07 (2012) 174.

[127] J. L. Bourjaily, N. Kalyanapuram, C. Langer, and K. Patatoukos, Prescriptive unitarity with elliptic leading singularities, Phys. Rev. D **104,** 125009 (2021).

[128] S. Abreu, R. Britto, C. Duhr, and E. Gardi, Algebraic Structure of Cut Feynman Integrals and the Diagrammatic Coaction, Phys. Rev. Lett. **119,** 051601 (2017).

[129] S. Abreu, R. Britto, C. Duhr, E. Gardi, and J. Matthew, The diagrammatic coaction beyond one loop, J. High Energy Phys. 10 (2021) 131.

[130] S. Abreu, R. Britto, C. Duhr, and E. Gardi, Cuts from residues: The one-loop case, J. High Energy Phys. 06 (2017) 114.

[131] J. L. Bourjaily, Y.-H. He, A. J. McLeod, M. von Hippel, and M. Wilhelm, Traintracks through Calabi-Yau Manifolds: Scattering Amplitudes beyond Elliptic Polylogarithms, Phys. Rev. Lett. **121,** 071603 (2018).

[132] J. L. Bourjaily, A. J. McLeod, M. von Hippel, and M. Wilhelm, Bounded Collection of Feynman Integral Calabi-Yau Geometries, Phys. Rev. Lett. **122,** 031601 (2019).

[133] J. L. Bourjaily, A. J. McLeod, C. Vergu, M. Volk, M. Von Hippel, and M. Wilhelm, Embedding Feynman integral (Calabi-Yau) geometries in weighted projective space, J. High Energy Phys. 01 (2020) 078.

[134] K. Bönisch, C. Duhr, F. Fischbach, A. Klemm, and C. Nega, Feynman integrals in dimensional regularization and extensions of Calabi-Yau motives, J. High Energy Phys. 09 (2022) 156.

[135] C. Duhr, A. Klemm, F. Loebbert, C. Nega, and F. Porkert, Yangian-Invariant Fishnet Integrals in Two Dimensions as Volumes of Calabi-Yau Varieties, Phys. Rev. Lett. **130,** 041602 (2023).

[136] S. Pögel, X. Wang, and S. Weinzierl, Taming Calabi-Yau Feynman Integrals: The Four-Loop Equal-Mass Banana Integral, Phys. Rev. Lett. **130,** 101601 (2023).

[137] C. F. Doran, A. Y. Novoseltsev, and P. Vanhove, Mirroring Towers: Calabi-Yau Geometry of the Multiloop Feynman Sunset Integrals (to be published).